Absolute light yield measurements on BaF_2 crystals and the quantum efficiency of several photomultiplier tubes*

P. Dorenbos, J.T.M. de Haas, R. Visser, C.W.E. van Eijk,
R.W. Hollander
Radiation Technology Group, Department of Applied Physics,
Delft University of Technology, Mekelweg 15, 2629 JB Delft, the Netherlands

Abstract

The quantum efficiency (QE) curves of five Philips XP2020Q photomultiplier tubes (PMTs), one Hamamatsu R2059 PMT, and a Na-Salicylate coated glass window were determined using a calibrated Thorn EMI 9426 PMT as a reference. The QE of XP2020Q PMTs at wavelengths smaller than 230 nm appears much better than the values specified by the manufacturer. Consequently, the often reported photon yield of 2000 photons/MeV for the fast component of the scintillation pulses from pure BaF_2 crystals determined with this tube is overestimated. Our results, obtained by means of calibrated equipment and using 662 keV γ-rays, yield a value of 1400 photons/MeV.

Introduction

The determination of the absolute photon yield of scintillation crystals can be rather troublesome especially in the far ultra-violet region of the electro-magnetic spectrum. Quantum efficiencies of photomultiplier tubes, optical transmission through window materials, ambient air, optical coupling compounds, or a monochromator should be accounted for. Absolute photon yields of scintillators were reported by Sakai [1] and Holl *et al.* [2]. They employed photodiodes or a photomultiplier tube with a borosilicate glass window. Both light detectors are, however, insensitive to the fast scintillation component, i.e. the cross-luminescence component, of BaF_2 which is emitted near 220 nm. A photomultiplier tube with a quartz window is needed to determine this fast photon yield. From the number of photoelectrons (phe) created in a PMT by a scintillating crystal within some time interval, the number of photons emitted per MeV of absorbed gamma ray energy in that time interval can be determined. In Table 1, we have compiled thus determined photoelectron yields of pure BaF_2 crystals which were reported in the literature since the discovery of the fast component of BaF_2 [3, 4].

Table 1: Gamma ray excited photoelectron yields/MeV reported in the literature for BaF_2 crystals coupled to a photomultiplier tube. In cases where several crystals were used, the average value was taken.

phe/MeV			
fast	total	PMT	reference
405[a)]	1900[c)]	XP2020Q	Laval *et al.* [3]
390[a)]	1940[c)]	XP2020Q	Moszynski *et al.* [5]
255[a)]	1600[c)]	R1668	Moszynski *et al.* [5]
445[a)]	2670[d)]	XP2020Q	Zhu *et al.* [6]
310[a)]	1465[d)]	XP2020Q	Chang *et al.* [7]
260[a)]	1580[e)]	XP2020Q	Klamra *et al.* [8]
184[b)]	1324[f)]	R2059	Woody *et al.* [9]

The following measuring techniques were employed. [a)]; a 10 ns differentiator followed by a fast stretcher. [b)]; charge integration during a 20 ns short gate. [c)]; spectroscopic techniques with a 6 μs shaping amplifier. [d)]; like [a)] but with a 6.5 μs differentiation time. [e)]; like [c)] but with a 2 μs shaping time. [f)]; like [b)] but with a 1 μs wide gate.

One observes a large variation in the number of phe/MeV of both the fast and the total yield. The reported fast yield varies between 260 and 445 phe/MeV if an XP2020Q PMT is used. The Hamamatsu R2059 and R1668 PMTs show the relatively low values of 184 and 255 phe/MeV. For the photon yield of the fast component of BaF_2, often the value of 2000 photons/MeV, originally reported by Laval *et al.* [3], is cited. Bruyndonckx *et al.* [10] reported a value of 2674 ph/MeV. In this work we find that these yields are overestimated: a value of 1400 photons/MeV is more likely. One reason is the quantum efficiency of the Philips XP2020Q PMT. Our measurements on this tube show that near 180 nm the QE is more than twice as good as the one specified by the manufacturer.

*These investigations in the program of the Foundation for Fundamental Research on Matter (FOM) have been supported by the Netherlands Technology Foundation (STW)

The latter, too low, quantum efficiency is usually applied to obtain the photon yield from the photoelectron measurements.

Experimental Results

Quantum efficiencies of PMTs

For measuring the quantum efficiency curves of several photomultiplier tubes and the x-ray excited emission spectra of BaF_2 crystals we employed an Acton Research Corporation (ARC model VM-502) vacuum ultraviolet monochromator. The monochromator has a 1200 grooves/mm concave reflection grating blazed in first order at 250 nm and was kept at a vacuum of 10^{-3} Pa. A 2.75 mm thick MgF_2 window is located in front of the entrance slit compartment of the monochromator. For measuring emission spectra, a sample cell containing the crystal is mounted in front of the MgF_2 window and kept at a vacuum of 0.1 Pa. x-rays from an x-ray tube with a Cu anode and operated at 35 kV and 25 mA enter the sample cell through a 0.3 mm thick Be window. Diaphragms inside the sample cell assure a well defined x-ray beam on the crystal. A photon detector is mounted behind the exit slit of the monochromator. In order to interpret a recorded emission spectrum correctly, the spectrum must be corrected for the quantum efficiency of the photon detector and the transmittance of the monochromator and window materials. Furthermore, a correction for possible second order transmissions through the monochromator should be made. Calibrated deuterium or tungsten lamps were placed in front of the entrance slit compartment in order to determine these properties.

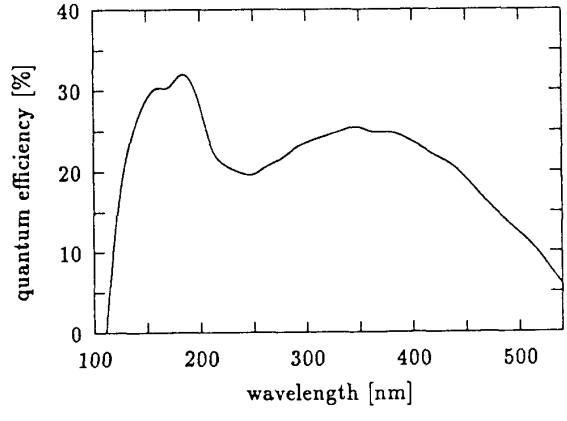

Figure 1: The quantum efficiency of the Thorn EMI 9426 photomultiplier tube (serial number 809).

To determine QE-curves of PMTs, we used a Thorn EMI 9426 PMT (Serial Number (SN) 809) with a MgF_2 window and a bi-alkali photocathode as a reference tube; its QE-curve is shown in Figure 1. The QE of our particular tube was measured by the manufacturer by means of light sources calibrated by the National Physics Laboratory England which in turn uses the Washington National Bureau of Standards reference standard photocells and thermopiles. In these measurements, the illumination of the photocathode was limited to a 16 mm diameter central circle. According to Thorn EMI, there is a systematic uncertainty in the quantum efficiency values of 10%. Light spectra of lamps and emission spectra of scintillation crystals measured with the EMI tube were compared with the spectra measured with the other photon detectors. Care was taken to avoid second order transmission through the monochromator. In cases when lamps are the light sources, quartz diffusers were applied to assure a homogeneous illumination of the monochromator's grating. The known QE curve of the EMI tube was then used to determine the shape of the QE curves of the others.

Three different types of photon detectors were tested:
i) Several Philips XP2020Q PMTs with a quartz window and a bi-alkali photocathode. A cathode-anode voltage, V_{k-a}, of -2100 V and a cathode-first dynode voltage, V_{k-d1}, of -500 V was supplied with a CERN type 4238 voltage divider network. The focalization and the V_{d1-d2} voltage was adjusted in order to obtain the optimal charge collection on the dynodes.
ii) A Hamamatsu R2059 PMT (SN: BA120) also with a quartz window and a bi-alkali photocathode. A V_{k-a} voltage of -2200 V was supplied with a standard Hamamatsu type 26 voltage divider network; V_{k-d1} = -720 V.
iii) A Na-salicylate coated glass window. Na-salicylate acts as a wavelength shifter for scintillation light below 340 nm and its emission light at 430 nm was detected by a Philips XP2020 PMT positioned closely behind the glass window. The Thorn EMI reference PMT was operated at a V_{k-a} voltage of -1700 V which was supplied with a Thorn EMI type H voltage divider network; V_{k-d1} = -214 V.

Figure 2a shows the obtained QE curve of one of the XP2020Q PMTs (SN:40161). The typical QE curve of the XP2020Q as specified by the manufacturer [11] is shown by the dashed curve. Since it was not possible to determine the absolute QE accurately, we have normalized the measured QE-curve in the wavelength region between 240 and 540 nm to this typical curve. Above 240 nm, both curves show the same shape. However, below 230 nm there is a large deviation. At these wavelengths, the QE of the photocathode appears to be much better than the one according to specifications. Four other XP2020Q PMTs (SN:18010, 18720, 40185, 40198) studied by us showed within 5% similar quantum efficiency curves. Like the EMI tube, the QE of the Philips tube increases as the wavelength decreases below 220 nm. In fact, the QE of the XP2020Q PMT is rather similar to that of the EMI tube except for the drop in QE near 165 nm caused by optical absorption in the quartz window of the PMT.

The QE curve of the Hamamatsu R2059 PMT measured

by us and the typical QE curve specified by the manufacturer [12] are shown in Figure 2b. Like for the XP2020Q and EMI 9426 PMTs, the QE increases when the wavelength drops below about 220 nm. This increase is however much less pronounced, and the QE near 190 nm is about a factor of two lower than the QE of the other two PMTs.

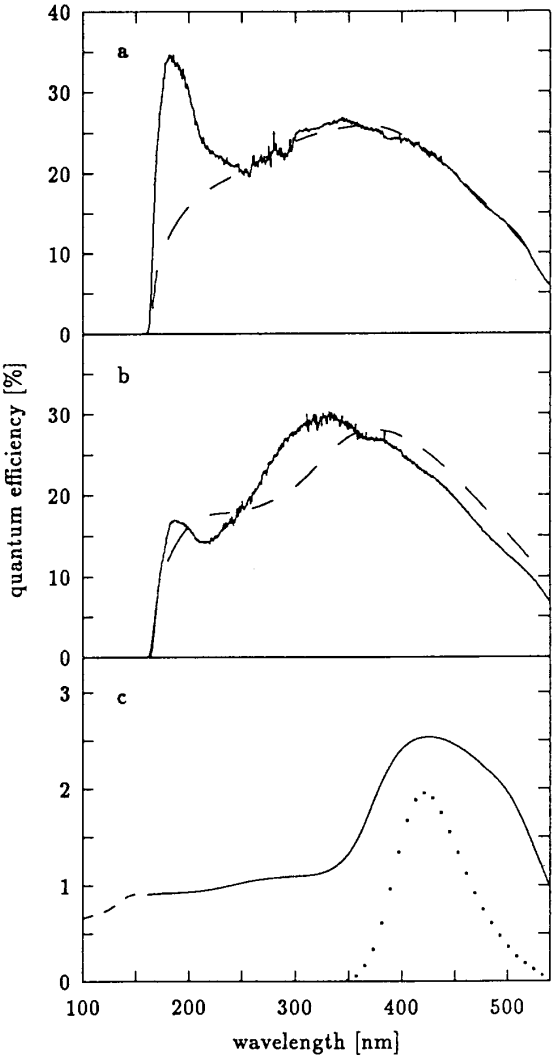

Figure 2: a) The solid curve shows the measured quantum efficiency (QE) of the Philips XP2020Q PMT (serial no. 40161), the dashed curve is the typical QE specified by the manufacturer [11]. b) QE of the Hamamatsu R2059 PMT (serial number BA120). The dashed curve shows the QE according to specifications [12]. c) QE of the Na-Salicylate coated glass window combined with an XP2020 PMT. The dashed curve is the extrapolated QE derived from [13]. The dotted curve shows the emission spectrum of Na-Salicylate.

Figure 2c shows the QE curve of the Na-salicylate coated glass window combined with the XP2020 PMT. The dashed curve between 100 and 160 nm is an extrapolation obtained from [13]. The emission spectrum of Na-Salicylate is also shown [14]. Photons with wavelength smaller than 340 nm are converted with a high efficiency of about 65% to 430 nm photons which are re-emitted isotropically [14]. Since the critical angle for total reflection in the glass window which is coated with the Na-Salicylate is 41.8°, only photons emitted within a solid angle of ≈ 1.6 sterad can be observed by the XP2020 PMT. The QE of the XP2020 PMT averaged over the emission band shape of Na-Salicylate is about 18%. Putting these numbers together, we expect an overall QE for the Na-Salicylate photon detector of about 1.5% at wavelengths smaller than 340 nm. This agrees, considering that we did not account for transmission and reflection losses in the Na-Salicylate coated glass window, with the observed value of about 1%. The rather constant QE between 180 and 240 nm corresponds well with literature [13, 14]. This provides a confirmation of the correctness of the large variations in QE of the EMI tube in this wavelength interval. At wavelengths above 340 nm, the Na-Salicylate becomes transparent and acts as a scatterer of incident light. The overall QE is then determined by this scattering action and the QE of the XP2020 PMT.

Absolute light yield of BaF_2 crystals

The scintillation properties of a 30 mm diameter and 6 mm thick pure BaF_2 crystal were determined by means of three techniques:

i) x-ray excited emission measurements
ii) scintillation decay measurements
iii) photoelectron yield measurements.

The crystal was manufactured by Harshaw, and all its sides were optically polished. The crystal shows an excellent optical transmission without absorption bands caused by unwanted impurities like e.g. Pb^{2+}. All experiments were performed at room temperature.

i) x-ray excited emission measurements: For x-ray excited emission measurements, the DC-current of the PMT was recorded as a function of the wavelength. The emission spectrum of the BaF_2 crystal must be corrected for the quantum efficiency of the PMT and the transmission of window materials and the monochromator. Above 190 nm, we have determined the transmission of the monochromator by means of a calibrated deuterium lamp and a calibrated tungsten lamp. The transmission is shown in Figure 3. The transmission as derived from the typical grating efficiency and the reflectivity of the aluminized mirrors in the VUV monochromator, which were specified by the manufacturer, is also shown. Both curves are normalized to one another. We employed the typical transmission to extrapolate the measured transmission towards lower wavelengths. The optical transmission of the MgF_2 window in front of the entrance slit compartment of the monochromator was measured with an Acton Research Corporation (model DS-775) deuterium light source.

The x-ray excited emission spectrum of the BaF_2 crys-

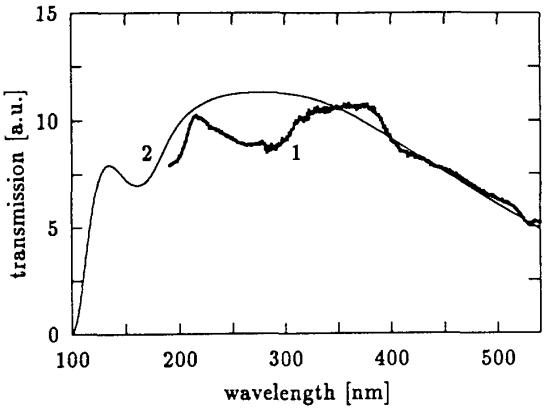

Figure 3: Curve 1: the transmission of the ARC VM-502 monochromator determined with calibrated lamps. Curve 2: typical transmission determined from the grating efficiency and the reflectivity of the aluminized mirrors.

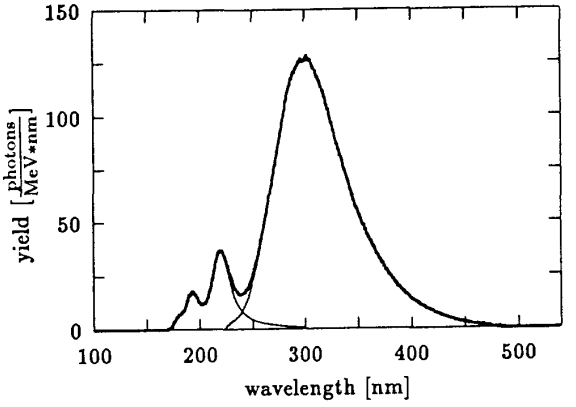

Figure 4: x-ray excited emission spectrum of pure BaF_2. The spectrum is corrected for the transmission and quantum efficiencies of the equipment used. The contributions of CL and STE luminescence to the spectrum are shown by the thin solid curves.

tal corrected for the transmissions and quantum efficiencies mentioned above is shown in Figure 4. The spectrum is also corrected for second order transmission through the monochromator. It is known that the fast component, caused by cross-luminescence (CL) with its emission bands at 175, 195, and 220 nm, has a low energy tail extending to beyond 300 nm [3, 15]. The slow emission component with its emission maximum near 300 nm is caused by self-trapped exciton (STE) luminescence. Integration of the CL and STE emission spectrum yields a fast to slow ratio of $1/(8.2\pm0.4)$. The ratio depends a little on the way the crystal is mounted in the sample cell which has probably to do with changes in the light collection efficiency. For reasons, to be justified later, we have normalized the integral of the CL emission spectrum to 1350 photons/MeV. The vertical scale in Figure 4 then represents the absolute number of photons/(MeV·nm) and the STE light yield equals about 11000 photons/MeV.

ii) Scintillation decay measurements: The decay of BaF_2 luminescence under 662 keV gamma ray excitation was determined by a modified version of the method of Bollinger *et al.* [16]. The BaF_2 crystal was mounted to the start PMT with an optical coupling compound. As stop PMT, we used the XP2020Q PMT (SN:40161) of which the quantum efficiency is shown in Figure 2a. The scintillation decay, corrected for random coincidences and dead time, is shown in Figure 5. From photoelectron yield experiments, to be discussed below, we were able to express the ordinate of the decay spectrum in absolute units of photoelectrons/(MeV·ns).

Roughly, we distinguish three time regimes. In regime I, cross-luminescence dominates which shows an exponential decay with a decay time of about 0.8 ns. The rise time of the fast CL pulse in the first 1.5 ns of the spectrum is determined by the time resolution of the set-up. From a study of the self-trapped exciton (STE) decay performed recently [17], we concluded that promptly created STEs are responsible for the decay observed in time region II. These STEs are created within a few hundred picosecond after absorption of a gamma photon and decay almost exponentially with a decay time of 630 ± 50 ns. The thin solid curve in Figure 5 shows this exponential decay. The measured decay curve deviates from the purely exponential decay curve in time region III. This is attributed to non-promptly created STEs. Trapped holes and trapped electrons diffuse through the crystal and recombine to form STEs in this time regime.

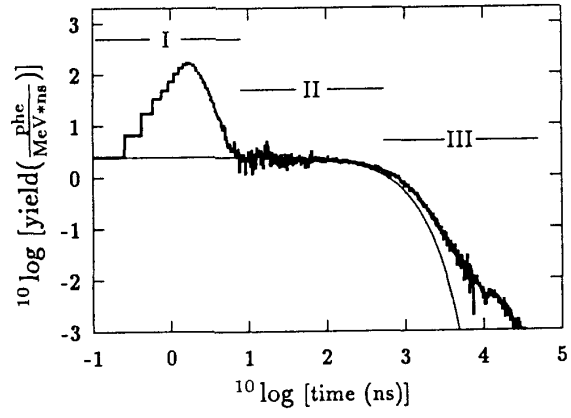

Figure 5: Scintillation decay spectrum of pure BaF_2. The spectrum is corrected for random coincidences and dead time. The thin solid curve shows an exponential decay with a decay time of 630 ns.

In the scintillation decay experiments, a photon emitted by the crystal must travel through about 10 cm of ambient

air before it can be detected by the stop XP2020Q PMT. The fast to slow ratio in a decay spectrum is therefore influenced by optical absorption in air and the QE of the stop PMT. The transmission of 10 cm of air was determined employing a D_2 lamp. There appears effectively a transmission cut-off at 185 nm. Correcting for these effects we obtain, by employing the spectral shape of the CL and STE luminescence spectra, a fast/slow ratio of $1/(6.9\pm0.2)$.

iii) Photoelectron yield measurements: The two methods described above provide the wavelength and time dependence of the BaF_2 scintillation light yield in arbitrary units. One of the very few ways to obtain the absolute photon yield is by means of photoelectron yield measurements. We mounted one side of the BaF_2 crystal to the window of a PMT with an optical coupling compound (General Electric Viscasil 60000 cSt), all other sides are covered by a few layers of 0.1 mm thick teflon tape. Viscasil and teflon cause on optimal light collection on the PMT photocathode [8, 18]. The crystal is irradiated with gamma rays from a ^{137}Cs source. Scintillation light pulses created in the scintillator cause photoelectron pulses in the PMT. From the 662 keV photopeak in the pulse height spectrum and from the *average* pulse height in the single electron pulse height spectrum of the PMT, the photoelectron yield is calculated. It should be noted that usually the position of the maximum in the single electron spectrum, i.e. the pulse height that occurs most frequently, is employed. This procedure is correct only if the single electron pulse height distribution is purely Gaussian which surely is not the case. Differences between the position of the maximum and the average pulse height can amount to 10 or 15%. A pre-amplifier and a Canberra (model 1413) shaping amplifier with a shaping time of 0.5 μs was used to obtain the single electron pulse height spectrum. The ^{137}Cs pulse height spectrum was determined for shaping times of 0.5, 1, 2, 4, 6, and 8 μs. The gain of the shaping amplifier was calibrated with an accuracy of 5%.

Figure 6a shows the obtained photo-electron yields/MeV of the BaF_2 crystal optically coupled to the XP2020Q PMT (SN:40161) as a function of the shaping time. Also shown are the photoelectron yields calculated from the scintillation decay spectrum in Figure 5. To obtain these yields we determined the response of the pre-amplifier and shaping amplifier combination to a sharp charge pulse which resembles a delta function input. The output of the shaping amplifier, with the scintillation pulse of BaF_2 as input, is then simulated by the convolution integral of the delta function response with this pulse. The calculated photo-electron yields presented in Figure 6a were determined using the scintillation decay spectrum in Figure 5 as the scintillation pulse. The calculated yields were normalized to the measured yields by a least squares method. From this normalization, the ordinate of the decay spectrum in Figure 5 in absolute units of photoelectrons/(MeV·ns) was obtained straightforwardly.

For the determination of the photoelectron yield of the fast and slow component separately, the anode pulses are

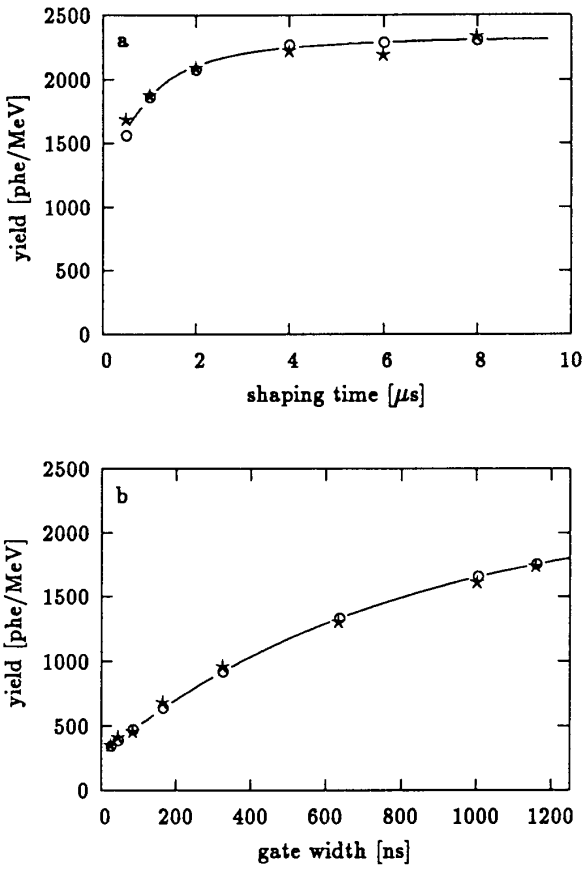

Figure 6: Photoelectron yields measured for the Ø30×6 mm BaF_2 crystal optically coupled to the XP2020Q PMT (SN:40161). a) ⋆, measured as a function of the shaping time. o, calculated from the scintillation decay curve. b) ⋆, determined with the LeCroy ADC as a function of the gate width. o, calculated from the scintillation decay curve. The solid curves are drawn to guide the eye.

fed to a LeCroy 2249W charge integrating ADC and to a constant fraction discriminator (CFD). The anode current is integrated by the ADC during the effective width of a gate pulse derived from the CFD output. The charge corresponding to the 662 keV photopeak is then proportional to the photoelectron yield within the time interval determined by the gate pulse. In order to obtain the proportionality constant, we first calculated the phe yield by simply integrating the scintillation pulse shown in Figure 5 during the effective width of the gate pulse. Next, the proportionality constant was obtained from a least squares fit of the charges corresponding to the 662 keV peaks to these calculated yields. The results are shown in Figure 6b.

The total photoelectron yield is obtained from the results in Figure 6 by extrapolation to infinite shaping times,

this gives 2400 phe/MeV. The fast component is obtained by extrapolation of the results obtained with the LeCroy ADC to zero gate width; this provides a fast yield of 290 phe/MeV. The yields obtained with the other four XP2020Q PMTs were within 5% similar to the values presented above. The photoelectron yield of the BaF_2 crystal was also determined with the Hamamatsu R2059 PMT, see Table 2. The fast photoelectron yield with the Hamamatsu R2059 PMT appears significantly less than the yield with the XP2020Q PMT.

Table 2: Results obtained from photoelectron yield measurements on a BaF_2 crystal performed with XP2020Q (SN:40161) and R2059 photomultiplier tubes. In addition to the stochastic errors in the compiled photon yields there is a possible systematic error of about 15%.

		XP2020Q	R2059
fast	(phe/MeV)	290 ± 15	195 ± 15
slow	(phe/MeV)	2110 ± 70	2280 ± 70
CL	(photons/MeV)	1430 ± 80	1380 ± 110
STE	(photons/MeV)	9500 ± 300	9400 ± 300

The photon yields calculated from the photoelectron yields are shown in Table 2. The following assumptions and corrections were made: i) because of the excellent reflection properties of Teflon and optical transmission of the BaF_2 crystal, we assumed a high light collection efficiency of about 92 %, ii) the yield of the fast component was corrected for the transmission cut-off of the optical coupling compound near 190 nm, iii) the results were corrected for the QE of the employed PMTs. We neglected possible variations of the QE with the angle of incidence of the incoming photons on the PMT window. Because of the assumptions made, there is an estimated systematic error of 15% in the compiled photon yields.

Discussion

The QE curve of the XP2020Q PMT differs significantly from the curve specified by the manufacturer (see Figure 2a). The measured QE increases if the wavelength drops below 240 nm whereas according to specifications the QE should decrease. The QE of the Hamamatsu R2059 PMT corresponds reasonably with specifications. Its QE below 220 nm is, however, significantly worse than that of the Philips XP2020Q and Thorn EMI 9426 PMTs. In a way Moszynski *et al.* [5] observed the same although they arrived at a different interpretation. These authors determined the phe yield/MeV of the fast component of BaF_2 with an XP2020Q PMT and several Hamamatsu R1668 PMTs. Except for a smaller diameter of 28 mm, the R1668 PMT is equivalent to the R2059 PMT which has a diameter of 50 mm. The Hamamatsu PMTs showed on the average a 40% lower phe yield than the XP2020Q PMT which agrees well with our observations. Assuming the correctness of the QE of the XP2020Q as specified by the manufacturer, they concluded that the collection efficiency of photoelectrons in the Hamamatsu PMT is worse, especially at wavelengths below 300 nm, than that of the XP2020Q PMT. Our results show, however, that it is not the *poor* collection efficiency of the Hamamatsu PMTs but the *good* QE of the XP2020Q PMTs which is responsible for the difference in photoelectron yield.

One might argue that the observed increase of the QE at wavelengths smaller than 240 nm is due to double photoelectron emission; i.e. one photon of sufficient energy creates two photoelectrons. In that case, the increase of the QE would not be a genuine increase but more like a wavelength dependent increase of the effective PMT's gain. However, from single photon pulse height spectra measured with the EMI tube under illumination of 185 nm photons, we conclude that at most 2% of the detected 185 nm photons create two photoelectrons. This number is too low to explain the observed QE increase at short wavelengths, and consequently double photoelectron emission is a rather unlikely explanation. The increase of the QE can be explained partly by assuming that a photon creates two kinetic electrons in the conduction band of the photocathode material. Though the probability that both electrons escape the photocathode is quite small, the probability that one of the two electrons escapes can be appreciable, resulting in a larger QE than if only one kinetic electron would have been produced.

Woody *et al.* [9] report a value of 184 phe/MeV for the fast component of pure BaF_2 with a R2059 PMT. With a technique similar to the one used by us, the anode pulse was integrated during a 20 ns wide gate pulse. This number still contains the contribution of the slow component within the 20 ns. Considering this contribution, their value is somewhat lower than our value of 195 phe/MeV. All the other fast phe/MeV values compiled in Table 1 were obtained with a different technique. The output pulse from the XP2020Q PMT was sent to a fast amplifier working with a 10 ns differentiation time constant and then to an integrating fast stretcher [3]. The gain of the PMT was determined from the single electron pulse height spectrum recorded with the same electronics. The fast component yield found in this way by Laval. *et al.*, Moszynski *et al.*, and Zhu *et al.* is about 400 phe/MeV. Chang *et al.* and Klamra *et al.* find values of 310 and 260 phe/MeV, respectively, which compare with the values found by us. The value of 400 phe/MeV seems rather large even after accounting for the presence of some slow component. Perhaps an underestimation of the gain of the PMT is responsible for this large value.

For the STE photon yield of the pure BaF_2 crystal, we obtain a value of about 9500±1400 photons/MeV. The error is caused by a possible 15% systematic error in the measured quantum efficiency of the PMTs employed and inaccuracies in the estimated light collection efficiency in photoelectron yield experiments. This photon yield compares with the values reported by Sakai [1] (11150 ph/MeV) and Holl *et al.* [2] (9950 ph/MeV).

Although corrections were made for quantum efficiencies and transmission losses, there remain still deviations in the fast/slow ratio determined by the three techniques. The smallest ratio, $1/(8.2 \pm 0.4)$, was observed with x-ray excited emission measurements, $1/(6.9 \pm 0.2)$ with scintillation decay measurements, and phe yield measurements gave $1/(6.8 \pm 0.6)$. In x-ray excited emission measurements, the PMT is operated in DC mode. Possible afterglow caused by delayed STE emission then also contributes to the emission spectrum which may explain the small fast/slow ratio. There is also the fact that the light yield of scintillators depends on the means of excitation. The difference in the fast/slow ratio is explained if the relatively low energy x-rays are either less efficient in producing cross luminescence or more efficient in producing STE luminescence than the 662 keV gamma rays. One aspect not considered in this work, is the light collection efficiency; the BaF_2 crystal is mounted differently in all three types of experiments which also may influence the fast/slow ratio.

The somewhat deviating fast/slow ratio in the x-ray excited BaF_2 emission spectrum limits the accuracy of the calibration of this spectrum in photons/(MeV·nm), see Figure 4. We have assumed an x-ray excited CL light yield of 1350 photons/MeV which then provides the absolute scale. By measuring emission spectra of scintillation crystals under identical conditions as used for the BaF_2 crystal, it is now possible to obtain an estimate for the absolute photon yields of these crystals with an accuracy of about 15%.

Summarizing, the QE of the XP2020Q PMT is at wavelengths smaller than 240 nm significantly larger than the QE as specified by the manufacturer. The difference amounts more than a factor 2 near 180 nm. Reported photon yields/MeV of scintillation emissions below 240 nm obtained employing this tube and its specified QE curve are overestimated significantly. In this work we obtain for pure BaF_2 at room temperature using 662 keV gamma rays, a CL light yield of 1400 ± 80 photons/MeV whereas a value of 2000 photons/MeV is often reported in the literature. The quantum efficiency of the Hamamatsu R2059 PMT appears at wavelengths below 240 nm about 40% worse than the QE of the XP2020Q and EMI 9426 PMTs.

References

[1] E. Sakai, "Recent measurements on scintillator-photodetector systems", *IEEE Trans. NS*, vol. 34(1), pp. 418-422, 1987.

[2] I. Holl, E. Lorenz, G. Mageras, "A measurement of the light yield of common inorganic scintillators", *IEEE Trans. NS*, vol. 35(1), pp. 105-109, 1988.

[3] M. Laval, M. Moszynski, R. Allemand, E. Cormoreche, P. Guinet, R. Odru, J. Vacher, "Barium fluoride - inorganic scintillator for subnanosecond timing", *Nucl. Instr. and Meth.*, vol. 206, pp. 169, 1983.

[4] N.N. Ershov, N.G. Zakharov, P.A. Rodnyi, "Spectral-kinetic study of the intrinsic-luminescence characteristics of a fluorite-type crystal", *Opt. Spektrosk. (USSR)*, vol.53(1), pp.51-54, 1982.

[5] M. Moszynski, R. Allemand, E. Cormoreche, M. Laval, R. Odru, J. Vacher, "Further study of scintillation counters with BaF_2 crystals for time-of-flight positron emission tomography in medicine", *Nucl. Instr. and Meth.*, vol.226, p.534-541, 1984.

[6] Y.C. Zhu, J.G. Lu, J. Li, Y.Y. Shao, H.S. Sun, B.Z. Dong, G.P. Zhou, Z.P. Zheng, F.Z. Cui, C.J. Yu, "New results on the scintillation properties of BaF_2", *Nucl. Instr. and Meth.*, A244 pp.577-578, 1986.

[7] T. Chang, D. Yin, C. Cao, S. Wang, J. Liang, "Improvement on application of BaF_2 scintillation counter to a positron lifetime spectrometer", *Nucl. Instr. and Meth.*, A256, pp.398-400, 1987.

[8] W. Klamra, T. Lindblad, M. Moszynski, L.O. Norlin, "Properties of optical greases for BaF_2 scintillators", *Nucl. Instr. and Meth.* A254, pp.85-87, 1987.

[9] C.L. Woody, P.W. Levy, J.A. Kierstead, "Slow component suppression and radiation damage in doped BaF_2 crystals", *IEEE Trans. NS*, vol.36, pp.536, 1989.

[10] P. Bruyndonckx, J. Debruyne, L. Etienne, M. Gruwé, B. Guerard, S. Tavernier, Z. Shuping, "BaF_2 scintillators with wire chamber readout for positron emission tomography", *Nucl. Instr. and Meth.*, vol. A310, pp.107-115, 1991.

[11] Data Handbook Photomultipliers, Philips Components, The Netherlands, Book PC04, pp.108, 1990.

[12] Hamamatsu brochure, Photomultiplier Tubes Dec/86.

[13] J.A.R. Samson, "Absolute intensity measurements in the vacuum ultraviolet", *J. of the Optical Soc. of America*, vol.54 no.1, pp.6-15, 1964.

[14] J.A.R. Samson, "Techniques of vacuum ultraviolet spectroscopy", *John Wiley and Sons*, New York, 1967.

[15] J.L. Jansons, V.J. Krumins, Z.A. Rachko, J.A. Valbis, "Luminescence due to radiative transitions between valence band and upper core band in ionic crystals (cross-luminescence)", *Phys. Stat. Sol. (b)*, vol.144, pp. 835, 1987.

[16] L.M. Bollinger, G.E. Thomas, "Measurements of the time dependence of scintillation intensity by a delayed-coincidence method", *Rev. Sci. Instr.*, vol. 32, pp. 1044, 1961.

[17] R. Visser, P. Dorenbos, C.W.E. van Eijk, H.W. den Hartog, "Energy transfer processes observed in the scintillation decay of BaF_2:La", to be published in *J. of Physics: Condensed Matter*, 1992.

[18] Z.Y. Wei, R.Y. Zhu, H. Newman, Z.W. Yin, "Light yield and surface treatment of barium fluoride crystals", *Nucl. Instr. and Meth.*, B61, pp.61-66, 1991.